Structural and optical characterization of epitaxial waveguiding $BaTiO_3$ thin films on MgO

L. Beckers, J. Schubert, W. Zander, J. Ziesmann, A. Eckau, P. Leinenbach, and Ch. Buchal

Citation: Journal of Applied Physics **83**, 3305 (1998);
View online: https://doi.org/10.1063/1.367099
View Table of Contents: http://aip.scitation.org/toc/jap/83/6
Published by the American Institute of Physics

Structural and optical characterization of epitaxial waveguiding $BaTiO_3$ thin films on MgO

L. Beckers, J. Schubert, W. Zander, J. Ziesmann, A. Eckau, P. Leinenbach, and Ch. Buchal[a)]
Institut für Schicht- und Ionentechnik (ISI), Forschungszentrum Jülich, D-52425 Jülich, Germany

(Received 23 June 1997; accepted for publication 26 November 1997)

Epitaxial waveguide structures of *c*-axis oriented $BaTiO_3$ thin films on MgO(001) have been grown by pulsed laser deposition. The structural properties of the samples have been characterized by Rutherford backscattering spectrometry/ion channeling (RBS/C), x-ray diffraction, and atomic force microscopy. We found excellent crystalline quality even up to thicknesses of a few microns. This has been confirmed by RBS/C minimum yield values of 2%–3%, a full width at half maximum of 0.36° of the $BaTiO_3$ (002) rocking curve, and a rms roughness of 1.1 nm for a 950 nm $BaTiO_3$ film. The out-of-plane refractive index was measured to be close to the extraordinary bulk value with the birefringence being about one third of the bulk value. Waveguide losses of 2.9 dB/cm have been demonstrated. © *1998 American Institute of Physics.* [S0021-8979(98)01206-7]

I. INTRODUCTION

There is strong interest to use crystalline optical materials in the form of thin films. The growth technology for some optical crystals, e.g., $LiNbO_3$, is very advanced, but a large variety of materials, such as $BaTiO_3$ and $KNbO_3$, are still very difficult to grow in large dimensions. An additional challenge is the formation of optical waveguides in the latter materials. Waveguides are essential for integrated optics. In particular, channel waveguides are needed for compatibility to optical fibers and for the formation of *Y* branches, Mach-Zehnder interferometers, etc. Thin films are useful for these applications. For the fabrication of thin films, pulsed laser deposition (PLD) is a very useful and flexible tool. PLD permits a stoichiometric transfer of material from the target to the film and film growth at high temperatures in reactive ambient gases, in particular, oxygen.[1] PLD has been very successful in the field of ceramic high temperature superconductors, such as epitaxial $YBa_2Cu_3O_{7-x}$ films, even for commercial applications.[2] At present, there is a wide variety of oxides being explored by thin film techniques. By growing thin films of these materials on readily available substrates, cost reduction and heterostructures with new functions can be achieved. We report the growth of thin films of barium titanate ($BaTiO_3$), a common ferroelectric perovskite. Its large electro-optic effect may be used in a Mach-Zehnder interferometer configuration. The bulk properties of $BaTiO_3$ in single crystal or polycrystalline form are well known.[3] Many groups have attempted to deposit $BaTiO_3$ as single crystalline films. Optical applications demand especially high crystalline quality because polycrystalline materials frequently show strong scattering. For heteroepitaxial growth, a suitable substrate has to be found. Due to its lower refractive index and its optical transparency, MgO is a very good substrate for $BaTiO_3$ waveguides. The lattice mismatch $m=(d_{\text{film}}-d_{\text{substrate}})/d_{\text{substrate}}$ between cubic MgO ($a=4.213$ Å, at 300 K) and tetragonal $BaTiO_3$ ($a=3.992$ Å; $c=4.036$ Å, at 300 K) is quite large ($BaTiO_3$ *a* axis: $m=-5.3\%$, $BaTiO_3$ *c* axis: $m=-4.2\%$). However, it is advantageous that the thermal expansion of MgO between the growth temperature and 300 K is similar to that of $BaTiO_3$ (Ref. 4). For the cooling process from 1000 °C to room temperature (see below), the linear contraction amounts to 1.4% for MgO and 1.25% for bulk $BaTiO_3$ (Ref. 4). This puts the $BaTiO_3$ film under some compressive stress for the in-plane directions and it favors a condition where the *c* axis of the $BaTiO_3$ in the tetragonal phase aligns itself perpendicular to the surface and the shorter *a* axes lie parallel to the surface.

The present article describes the growth of single-crystalline $BaTiO_3$ films by the PLD process. First, we discuss the structural properties of the films. Subsequently, the optical results are presented. $BaTiO_3$ films of different thickness have been analyzed, and a consistent picture of film growth and properties is presented. If compared to recently published data of $BaTiO_3$ waveguides on MgO grown by metalorganic chemical vapor deposition (MOCVD),[5] the smoothness of our PLD films is significantly improved.

II. EXPERIMENT

The PLD setup uses a KrF excimer laser (248 nm, 40 ns, 10 Hz, $2-4$ J/cm^2) and has been described in detail.[6] The cylindrical target consists of single phase $BaTiO_3$ powder which has been pressed and sintered. The MgO(001) substrates, with dimensions $10\times10\times1$ mm^3, are placed on a resistive SiC heater inside the PLD chamber. The MgO substrates have been purchased from a commercial supplier.[7] They are chemomechanically polished and are specified as ''epitaxial grade'' with a rms roughness of 1.5 nm or better. In the PLD chamber, they are heated in vacuum to the deposition temperature and are given time to equilibrate with the heater for 5 min. Then the deposition process takes place under an oxygen pressure ranging from 1×10^{-3} to 5

a)Electronic mail: c.buchal@fz-juelich.de

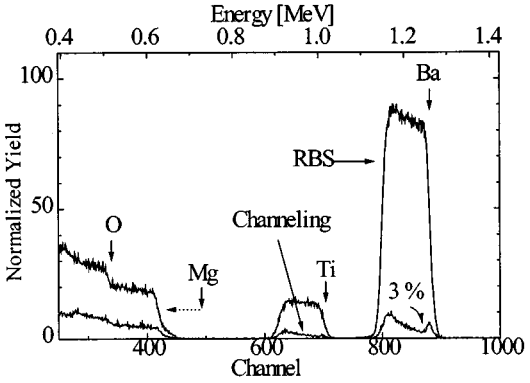

FIG. 1. RBS/ion channeling spectra of a 115 nm thick $BaTiO_3$ film on MgO.

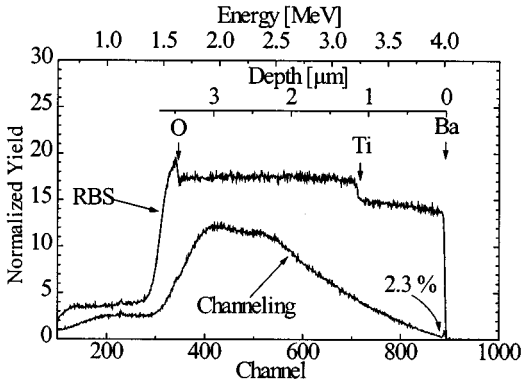

FIG. 2. RBS/ion channeling spectra of a 3.7 μm thick $BaTiO_3$ film on MgO, measured with 4.5 MeV He^{++} incident energy.

$\times 10^{-1}$ mbar and a substrate temperature of up to 1200 °C. As optimum parameters we found a temperature of approximately 1000 °C at an oxygen pressure of 4×10^{-3} mbar. To improve the film properties, an *in situ* annealing step has been included: directly after completing the deposition process, the chamber was flooded with oxygen and the sample was annealed for 3 min in 1000 mbar oxygen. Typical deposition rates were 1–5 nm/s. Structural characterization was performed by Rutherford backscattering spectrometry/ion channeling (RBS/C), x-ray diffraction (XRD), and atomic force microscopy (AFM). For the optical measurements, a prism coupling setup similar to that of Walker *et al.*[8] was used. By rotating the sample, different optical modes can be excited in the $BaTiO_3$ film by a He–Ne laser (wavelength 632.8 nm), which was coupled into the film by a rutile prism. If the film guides two or more modes, a least mean square fit was used to calculate the refractive index and the thickness of the film. A substrate refractive index of 1.734 ± 0.001 was determined from the substrate mode. The setup permits the measurement of the two in-plane and the out-of-plane refractive indices of the films. To determine waveguide losses, the position dependence of the light scattered from the film was measured by a greyscale charge coupled devise (CCD) video camera (Model Pulnix TM 6-CN) and digitally recorded for analysis.

III. RESULTS AND DISCUSSION

A. Structural characterization

The $BaTiO_3$ films were first characterized by Rutherford backscattering spectrometry/ion channeling. Figure 1 shows the spectra from a $BaTiO_3$ film on MgO after deposition and subsequent annealing under optimum conditions as mentioned above. The energy of the incident He^+ ions was 1.4 MeV. The simulation of the RBS spectrum verifies the stoichiometric composition of the deposited $BaTiO_3$ and gives a layer thickness of 115 nm. The Ba/Ti ratio was determined to be 0.998, in accordance with the initial target composition. The oxygen concentration in the films is more difficult to determine by RBS, because of the low atomic mass of oxygen. The sharp edges of the barium and titanium signals are indicative of good film thickness uniformity. No evidence for interdiffusion between the film and the substrate was found. Compared to the spectrum taken in a random direction, the aligned spectrum shows a strong decrease in backscattering yield, indicating high crystalline quality. The minimum yield χ_{min} is 3%, which is a typical result obtained from single crystals.[9] The aligned signal shows a gradual increase towards lower energies, which may be attributed to a thin distorted layer within the $BaTiO_3$ film close to the MgO interface.

Remarkably, the same high crystalline quality ($\chi_{min} \leqslant 3\%$) is observed for $BaTiO_3$ films of different thickness, even for a few microns thickness. For analyzing these thick films, higher He ion energies have to be used. Figure 2 shows the spectra from an approximately 3.7 μm thick $BaTiO_3$ film on MgO. The He energy was 4.5 MeV. From energy loss data determined with help of the TRIM code,[10] a depth scale for the barium signal is calculated. A simulation of the RBS spectrum verifies the stoichiometric composition of the $BaTiO_3$ film within the experimental errors. The same film was also analyzed at 1.4 MeV He energy (not shown), confirming the stoichiometric composition of the top 1 μm of the film. The minimum yield values at 1.4 and 4.5 MeV are 1.8% and 2.3%, respectively. We thus conclude that the 3.7 μm $BaTiO_3$ film is single crystalline over the whole depth. Compared to results of other groups, the crystalline quality of our samples is very good. Scarfone *et al.*[11] found $\chi_{min}=20\%$ in 70 nm thick $BaTiO_3$ films on MgO. Values as low as $\chi_{min}=1.7\%$ have only been observed for $BaTiO_3$ on the structurally similar $SrTiO_3$ substrates by Gong *et al.*[12] In good agreement with this reference, we have observed χ_{min} values around 2% for $BaTiO_3$ films deposited on $SrTiO_3$. The deposition parameters for films on $SrTiO_3$ were the same as those on MgO. For $BaTiO_3$ films on the more optically desirable substrate MgO, χ_{min} values which are comparable to perfect crystals have not been reported previously to our knowledge.

In addition to RBS/C XRD measurements were performed. The $\Theta/2\Theta$ scan of the 3.7 μm thick $BaTiO_3$ film on MgO is shown in Fig. 3. In addition to the (002)- and (004)-peaks of the substrate, four reflections appear which can be indexed as the $(00n)$ planes of $BaTiO_3$. No peak splitting was found. The calculated film lattice parameter of 4.031 Å is close to the *c*-axis parameter of tetragonal $BaTiO_3$. By tilting the sample at a fixed angle during a conventional $\Theta/2\Theta$ scan, the lattice spacing of the (103) planes can be

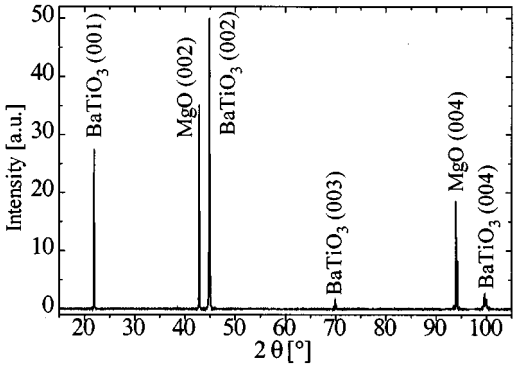

FIG. 3. $\theta/2\theta$ XRD scan of a 3.7 μm thick $BaTiO_3$ film on MgO.

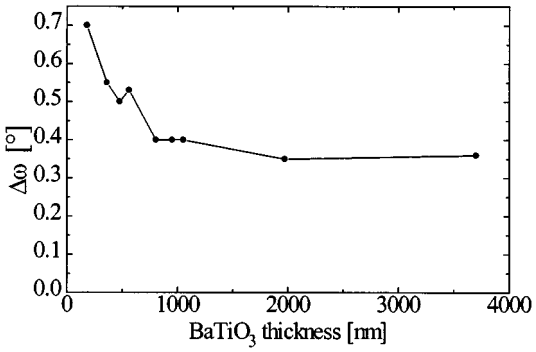

FIG. 5. Full width at half maximum (FWHM) $\Delta\omega$ of the rocking curve of the (002) $BaTiO_3$ reflection, plotted for different samples vs their $BaTiO_3$ film thickness.

measured. Hence, the lattice constant parallel to the surface can be calculated. For the film shown in Fig. 3, an in-plane value of 4.006 Å has been estimated. A pole figure scan (not shown) on the (103) $BaTiO_3$ reflection displays the expected fourfold symmetry, which is aligned parallel to the (103) MgO direction.

To determine the thickness dependence of the lattice constants, a series of samples was measured and the results are shown in Fig. 4. The lattice parameter perpendicular to the surface is nearly independent of the film thickness and is close to the *c*-axis bulk value. For the thinnest films, the in-plane value is intermediate between the bulk *a*- and *c*-axis values; the in-plane value approaches the bulk *a*-axis value with increasing film thickness.

At present, there is no complete and conclusive description of the growth process, but some very helpful ideas shall be presented.[13,14] Srikant *et al.* studied the growth of $BaTiO_3$ films on different substrates.[13] They conclude that at high temperatures the films grow in the cubic phase and always accommodate the misfit to the substrate by dislocations. Then, on cooling, the film deforms elastically to compensate the thermal mismatch with the substrate and the net strain dictates the orientation of the tetragonal $BaTiO_3$ film.[13]

For our experiments, we have to consider the linear thermal expansion of MgO and of $BaTiO_3$ (Ref. 4). Our best films are grown at 1000 °C. When being cooled to 130 °C, the MgO substrate shrinks by $\Delta l/l = 1.27\%$, while bulk $BaTiO_3$ would shrink by $\Delta l/l = 1.17\%$. For the thin epitaxial $BaTiO_3$ film, this results in a compressional strain $\epsilon_{II} = 0.1\%$, corresponding to an in-plane shortening of the $BaTiO_3$ *a* axes of 0.004 Å. At $T_c = 125 \pm 5$ °C, bulk $BaTiO_3$ undergoes the phase transition from the cubic to the tetragonal phase. At this transition, the *a* axes contract by approximately 0.005 Å and the *c* axis expands by approximately 0.012 Å.[3,15]

Therefore at $T < T_c$, the thermal stress and the resulting strain are completely compensated by the tetragonal distortion, if the $BaTiO_3$ *c* axis orients itself perpendicular to the film surface. As Ref. 15 shows for bulk $BaTiO_3$, further cooling from T_c to room temperature would result in an additional contraction of the *a* axes by 0.011 Å. From Ref. 4 it follows that the MgO substrate contracts by 0.005 Å over this temperature span, leaving the $BaTiO_3$ film now under tensile stress. As a consequence, the in-plane lattice parameters for the $BaTiO_3$ films are consistently larger than the bulk value. This is shown in Fig. 4. From Poisson's law we expect a shortening of the *c* axis. Assuming for Poisson's ratio $\mu \approx 0.3$ (a fair guess for this class of materials), we find $\Delta 1 = -0.005$ Å, in agreement with our data. Whereas these statements hold well for films of thicknesses exceeding 500 nm, thinner films show a very strong tensile strain of the *a* axes, which we cannot quantitatively explain at present.

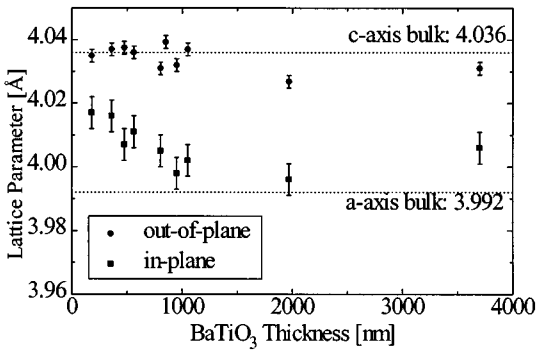

FIG. 4. Lattice constants in plane and out of plane for various film thicknesses. Also indicated are the bulk values of tetragonal $BaTiO_3$ at room temperature.

Additional information can be extracted from x-ray diffraction by measuring the rocking curves of the $BaTiO_3(00n)$ reflexes. The same series of samples, as shown in Fig. 4, has been investigated and the full width at half maximum (FWHM), measured at the (002) reflection, is plotted versus film thickness in Fig. 5. It can be seen that the width of the rocking curve decreases with increasing film thickness and levels out at a constant value of 0.35–0.4° at a film thickness >1 μm. In general, the rocking curves are very narrow and indicate well-oriented $BaTiO_3$ films. The higher values for the thinner films suggest that part of the $BaTiO_3$ film near the interface is misaligned.

In addition to the crystalline quality, the surface morphology of the films is very important for waveguide applications. A rough surface leads to scattering losses. Fork *et al.*[16] estimate for a similar material, that the surface rms roughness needs to be of the order of 1 nm or below. To measure the surface roughness, some samples were analyzed

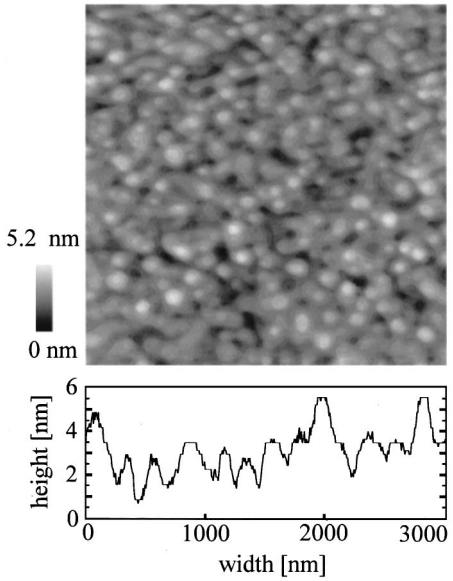

FIG. 6. Atomic force microscopy (AFM) picture taken from a 950 nm $BaTiO_3$ film on MgO.

by AFM. Figure 6 shows an image of a $3\times3\ \mu m^2$ area of a 950 nm $BaTiO_3$ film. The surface is very flat; only some small islands are visible. In the lower part of Fig. 6, a line scan has been extracted from the image. The maximum variation in height [peak-to-valley (PV) roughness] is 5.2 nm. The rms roughness was evaluated to be 1.1 nm. This is only 0.1% of the deposited thickness and is therefore quite low. For samples of a smaller $BaTiO_3$ film thickness, even lower roughness values were found. The AFM measurements suggest that no significant contribution to waveguide losses is expected from the surface morphology.

To resolve the domain structure, the $BaTiO_3$ films have been analyzed using an optical microscope with crossed polarizers. In this configuration, no structure in the films and therefore no domains with the *c* axis lying in plane can be observed. To detect domain regions with reversed *c* axis perpendicular to the film surface, some films have been etched in 37% HCl for up to 20 min at room temperature, following Hooton and Merz.[17] $BaTiO_3$ shows a distinct difference in etch rate between the positive and the negative face of the ferroelectric domains. Therefore a domain pattern results in an etch pattern, which can be observed under an optical microscope. No domain structure was found. From this and the formerly presented structural information, we conclude that the films consist of a single *c* domain. This result can be explained by the self-poling phenomenon, which was introduced by Marx *et al.*[18] They observed poled regions near the surface of a barium strontium titanate niobate (BSTN) crystal, even when the crystal was heated above the Curie temperature. In their experiment, the self-poling is induced by the strain from a deposited SiO_2 film. In our case, this should be caused by the substrate. As discussed above, the *c* orientation is favored to minimize the strain. Investigations of the samples with cross-sectional transmission electron microscopy will give further insight into the film structure.

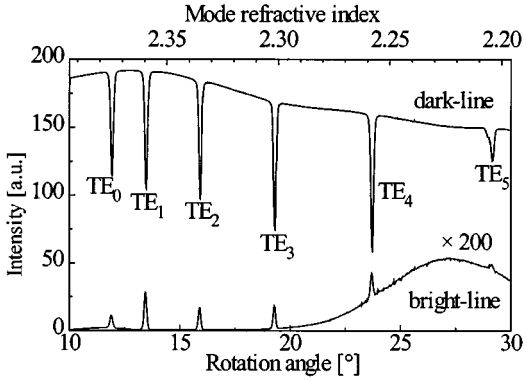

FIG. 7. Dark-line and bright-line spectrum of the TE_0-TE_5 modes in a 2 μm thick $BaTiO_3$ film.

B. Optical characterization

In the previous section, the high crystalline quality of the films has been demonstrated. For waveguide applications, optical measurements are necessary. Waveguide losses are sensitive to a number of factors such as surface and interface roughness and internal scattering.[16] Figure 7 shows the intensity of the dark-line and the bright-line detector versus the rotation angle of the goniometer, which is a measure of the mode refractive index. There are six sharp dips in the dark-line spectrum, corresponding to peaks in the bright-line spectrum at the same positions. Note that the bright-line spectrum is scaled by a factor of 200. The low intensity reaching the bright-line detector is explained by the fact that no end face polishing was provided. From Fig. 7 the mode refractive index is calculated. The incident light was polarized parallel to the surface, so the positions can be identified as the TE_0-TE_5 modes. Although the entrance position of the laser beam spot into the prism was carefully adjusted according to a method proposed by Ulrich and Torge,[19] only a limited angular interval can be scanned. The laser spot moves on the base plane of the prism and causes the broad peak in the bright-line spectrum of Fig. 7 by reaching the edge of the prism. For the subsequent TE_6-TE_8 modes, a new adjustment is necessary. If all modes were measured, the refractive index was determined to be 2.378 ± 0.002 and the waveguide thickness to be 2020 ± 10 nm. These calculations assume a rectangular refractive index profile and a homogeneous $BaTiO_3$ film index.

Using this procedure, the refractive indices of a series of samples were measured and plotted in Fig. 8. The deposition parameters for all samples were identical, only the deposition time and therefore the thickness was varied. For all samples, a birefringence in the films is clearly visible, resulting in two different refractive indices for the two orthogonal polarizations TE and TM. The lower indices were found for the TM modes (electrical field perpendicular to the surface). The absolute value agrees reasonably well with the extraordinary index n_e (or n_c) of bulk $BaTiO_3$ crystals. Higher refractive indices were observed for the TE modes. Both indices increase slightly with increasing film thickness, but the difference remains constant at $\Delta n\approx0.014$. This value agrees with the findings of Kim and Kwok,[20] who also used PLD to

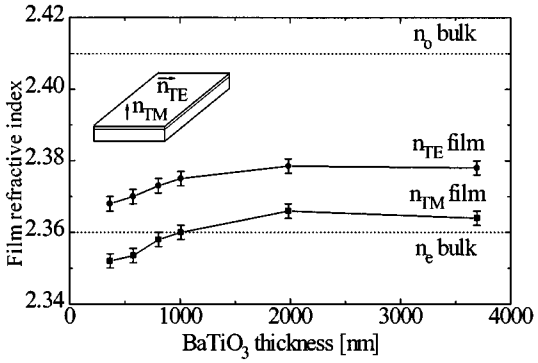

FIG. 8. In-plane and out-of-plane indices plotted for a series with various thicknesses. The straight line is a guide for the eye. The dotted lines indicate the $BaTiO_3$ bulk values.

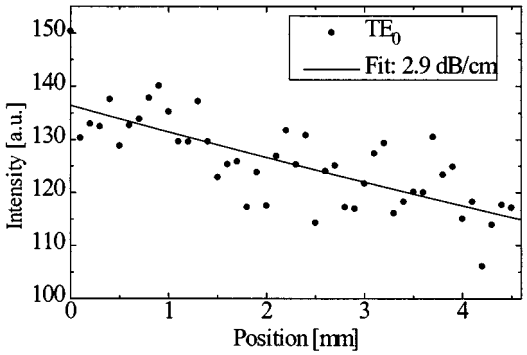

FIG. 9. Scattered intensity from the TE_0 mode for a 600 nm $BaTiO_3$ film on MgO. The best exponential fit results in a loss of 2.9 dB/cm.

deposit $BaTiO_3$ films on MgO. An explanation for the decrease of both indices in Fig. 8 could be the existence of a disturbed region with lowered refractive index in the $BaTiO_3$ film near the interface. The influence of this region on the averaged refractive index of the film decreases with film thickness. Usually a disordered perovskite crystal has a lower index.[21] For the TE measurements, a rotation of the sample by 90° or 45° results in the same index, showing that the in-plane index is homogeneous. These indices are below the ordinary indices of bulk $BaTiO_3$.

The data of Fig. 8 show one optical axis perpendicular to the surface, similar to bulk tetragonal $BaTiO_3$. The birefringence is about one third of the bulk value. As the films appear very homogeneous and free of domains, the results from Fig. 8 can be easily understood: the out-of-plane lattice parameter and hence the refractive index are the same as for the *c* axis in bulk $BaTiO_3$. As we have shown, this direction nearly assumes the bulk value. In contrast, the in-plane lattice parameter is more strongly influenced by the MgO substrate. This results in a lengthening of this axis and in a decrease of the refractive index. This indicates, that with increasing distance between the ions in the $BaTiO_3$, polarizability and refractive index decrease. Experimental values of the strain-optic coefficient, which describes the change of refractive index due to compressional or tensile strain, are not available for $BaTiO_3$ to our knowledge. Nevertheless, our observations are in agreement with the findings of Refs. 18 and 22. They have shown that compressional strain enhances the refractive index in $LiNbO_3$, $LiTaO_3$, $BaTiO_3$ and BSTN.[18,22]

Figure 9 shows the measured scattered intensity from a waveguide as a function of propagation along the guide. The TE_0 mode in a 600 nm thick $BaTiO_3$ film on MgO was excited and the data were extracted from a digitally recorded picture. A reduction in scattered light intensity along the length of this planar waveguide can be observed. If we assume that the scattered light intensity is proportional to the total light intensity inside the guide, the waveguide losses can be determined. This assumption is correct for homogeneous waveguides, which the planar $BaTiO_3$ film appears to be from the structural data. From the data shown in Fig. 9, a loss of 2.9 dB/cm can be evaluated. Especially for low losses, the accuracy of this method is limited, but it gives a good approximation. It may be compared to the value of 3 dB/cm, published by Walker *et al.* in molecular beam epitaxy (MBE) grown $SrTiO_3$ films on MgO[8] and to 4 ± 2 dB/cm, as achieved by MOCVD for $BaTiO_3$ films.[5] For the TE_0 and TM_0 modes, values in the range of 3 dB/cm were typical and found in different films. For modes of higher order we determined higher losses.

Future investigations will go towards channel waveguides and the fabrication of a Mach-Zehnder interferometer.

IV. CONCLUSIONS

In conclusion, single crystalline *c*-oriented $BaTiO_3$ films were deposited on the technologically interesting substrate MgO. The films showed very low χ_{min} values, narrow rocking curves, and very flat surfaces. No deterioration of the crystalline structure with increasing film thickness has been observed up to a few microns. Corresponding to the structural investigations, the optical properties were found to be very promising. We observed birefringent films with the optical axis perpendicular to the surface and waveguide losses of 2.9 dB/cm. So far, the tetragonal distortion (determined by x-ray diffraction) as well as the birefringence of the films is lower than that of bulk $BaTiO_3$. The fabrication of integrated optical devices is in progress.

ACKNOWLEDGMENTS

The authors gratefully acknowledge the support from the Tandetron facility and staff at IFF of Forschungszentrum Jülich. This work has been supported by the ESPRIT Long Term Research Project No. 21838 SCOOP (Silicon Compatible Optoelectronics).

[1] D. H. Lowndes, D. B. Geohegan, A. A. Puretzky, D. P. Norton, and C. M. Rouleau, Science **273**, 898 (1996).
[2] Y. Zhang, Y. Tavrin, H. J. Krause, H. Bousack, A. I. Braginski, U. Kalberkamp, U. Matzander, M. Burghoff, and L. Trahms, Appl. Suppercond. **3**, 367 (1995).
[3] J. Harada, in *Landolt-Börnstein, Ferroelektrika und verwandte Substanzen, The New Series III 16 a* (Springer, Berlin, 1981), p. 66 ff.
[4] Y. S. Touloukian, R. D. Kirby, R. E. Taylor, and T. Y. R. Lee, *Thermophysical Properties of Matter* (Plenum, New York, 1977) Vol. 13, p. 288 (MgO), p. 554 ($BaTiO_3$).
[5] D. M. Gill, B. A. Block, C. W. Conrad, B. W. Wessels, and S. T. Ho, Appl. Phys. Lett. **69**, 2968 (1996).

[6] B. Stritzker, J. Schubert, U. Poppe, W. Zander, U. Krüger, A. Lubig, and Ch. Buchal, J. Less-Common Met. **164,165**, 279 (1990).
[7] Crystec GmbH, Köpenicker Str. 325, D-12555 Berlin, Germany.
[8] F. J. Walker, R. A. McKee, H.-W. Yen, and D. E. Zelmon, Appl. Phys. Lett. **65**, 1495 (1994).
[9] L. C. Feldman, J. W. Mayer, and S. T. Picraux, *Materials Analysis by Ion Channeling* (Academic, New York, 1982).
[10] J. P. Biersack and L. G. Haggmark, Nucl. Instrum. Methods **174**, 257 (1980); ''TRIM'' is a computer code provided by these authors.
[11] C. Scarfone, M. G. Norton, C. B. Carter, J. Li, and J. W. Mayer, Mater. Res. Soc. Symp. Proc. **201**, 183 (1991).
[12] J. Gong, M. Kawasaki, K. Fujito, U. Tanaka, N. Ishizawa, M. Yoshimoto, H. Koinuma, M. Kumagai, K. Hirai, and K. Horiguchi, Jpn. J. Appl. Phys., Part 1 **32**, L687 (1993).
[13] V. Srikant, E. J. Tarsa, D. R. Clarke, and J. S. Speck, J. Appl. Phys. **77**, 1517 (1995).
[14] Y. Yoneda, H. Kasatani, H. Terauchi, Y. Yano, T. Terashima, and Y. Bando, J. Cryst. Growth **150**, 1090 (1995).
[15] H. F. Kay and P. Vousden, Philos. Mag. **40**, 1019 (1949).
[16] D. K. Fork, F. Armani-Leplingard, and J. J. Kingston, Mater. Res. Soc. Symp. Proc. **361**, 155 (1994).
[17] J. A. Hooton and W. J. Merz, Phys. Rev. **98**, 409 (1955).
[18] J. M. Marx, O. Eknoyan, H. F. Taylor, Z. Tang, and R. R. Neurgaonkar, Appl. Phys. Lett. **67**, 1381 (1995).
[19] R. Ulrich and R. Torge, Appl. Opt. **12**, 2901 (1973).
[20] D. H. Kim and H. S. Kwok, Appl. Phys. Lett. **67**, 1803 (1995).
[21] Ch. Buchal, Nucl. Instrum. Methods Phys. Res. B **96**, 370 (1995); Ch. Buchal, S. P. Withrow, C. W. White, and D. B. Poker, Annu. Rev. Mater. Sci. **24**, 125 (1994).
[22] O. Eknoyan, H. F. Taylor, Z. Tang, V. P. Swenson, and J. M. Marx, Appl. Phys. Lett. **60**, 407 (1992).